Classification: Biological Sciences: Evolution

The historical demography of Müllerian mimicry in the Neotropical *Heliconius* butterflies

Nicola S. Flanagan, Alexandra Tobler*, Angus Davison[†], Oliver G. Pybus[‡], Durrell D. Kapan, Silvia Planas, Mauricio Linares[§], David Heckel[¶], and W. Owen McMillan

Department of Biology, University of Puerto Rico, PO Box 23360, San Juan, Puerto Rico 00931-3360.
* Current Address: Department of Biology, Duke University, Durham, NC 27708
[†] Current Address: ICAPB, Ashworth Laboratories, West Mains Road, University of Edinburgh, Edinburgh, EH9 3JT. UK
[‡] Dept of Zoology, University of Oxford, South Parks Rd, Oxford, OX1 3PS, UK
[§]Instituto de Genética, Universidad de los Andes, PO Box 4976, Santafé de Bogotá, República de Colombia
[¶] Department of Genetics, The University of Melbourne, Parkville, Victoria, 3052 Australia

Corresponding author: Nicola S. Flanagan. Dept. of Biology, University of Puerto Rico, PO BOX 23360, SAN JUAN PR 00931-3360. Tel: +61-2-62592035. Fax: +1-787-764-3875. Email: nicflanagan@fastmail.fm

Manuscript information:
No. of text pages: 18
No. of figures: 2
No. of tables: 2
No. of words in abstract: 236
Total no. of characters: 46,803
Abbreviations footnote: *Mannose phosphate isomerase, Mpi*; *Triose phosphate isomerase, Tpi*; Maximum likelihood, ML; Time to most recent common ancestor, TMRCA.

Data deposition footnote: All sequences have been submitted to Genbank, accession numbers; AF413720, AF413723-AF413725, AF413728, AF413726, AF413739, AF413743, AF413744, AF413758, AF413752-AF413755, AF413758, AF413764, AF413770, AF413782, AF413783, AF413785-AF413787, AF413789, AF413790, AY319192-AY319254; AY319856-AY319923; AY329801-AY329843; AY332412-AY332464.

Abstract

We compare the historical demographies of two Müllerian co-mimetic butterfly species, *Heliconius erato* and *H. melpomene*. These species show an extensive parallel geographic divergence in their aposematic wing phenotypes. Recent studies suggest that this coincident mosaic results from simultaneous demographic processes shaped by extrinsic forces over the Pleistocene climate fluctuations. However, DNA sequence variation at two rapidly evolving unlinked nuclear loci, *Mannose phosphate isomerase* (*Mpi*) and *Triose phosphate isomerase* (*Tpi*) show the co-mimetic species to have quite different Quaternary demographies. In *H. erato,* despite ongoing lineage sorting across the Andes, nuclear genealogical estimates show little geographical structure, suggesting high historical gene flow. Coalescent-based demographic analysis reveals population growth since the Pliocene. Although these patterns suggest vicariant population subdivision associated with the Andean orogeny, they are not consistent with hypotheses of Pleistocene population fragmentation facilitating allopatric wing phenotype radiation in *H. erato*. In contrast, nuclear genetic diversity, θ, in *H. melpomene* was reduced relative to its co-mimic and revealed three phylogeographical clades. The pattern of coalescent events within regional clades is most consistent with population growth in relatively isolated populations, following a recent period of restricted population size. These different demographic histories suggest that the wing pattern radiations were not coincident in the two species. Instead, larger N_e in *H. erato,* together with profound population change in *H. melpomene* supports an earlier hypothesis that the former diversified first as the model species of this remarkable mimetic association.

Introduction

The neo-tropical butterflies *Heliconius erato* and *H. melpomene* are an exceptional example of Müllerian mimicry. These distantly related (1, 2), unpalatable species have both radiated into almost 30 wing phenotypic races. However, in any one location across their sympatric ranges, they exhibit near perfect convergence in their warningly-colored wing patterns. This parallel diversification argues forcefully for the adaptive nature of the mimicry between the two species, and strong stabilizing selection on local patterns has been demonstrated (3, 4).

Nonetheless, the origins of this coincident mosaic of divergence and convergence remain highly controversial (5, 6). Under Müllerian mimicry theory strong frequency-dependent selection should promote convergence to a single common wing pattern at both intra- and inter-specific levels. One explanation is closely allied with the 'Pleistocene refugia model' for the evolution of diversity in Amazonia (7). The so-called 'Brown-Sheppard-Turner' model (8, 9) proposes that the two species underwent simultaneous population constrictions during the Pleistocene climatic perturbations, with each mimetic racial pair originating in response to stochastic changes in the biotic environment in isolated populations. Based on cladograms of the two radiations constructed from allelic changes in major wing patterning loci, Sheppard and co-workers (8) further suggested that similar wing pattern races within a species were most closely related, despite often being geographically separated by other, phenotypically-distinct races. Matching pattern gene cladograms may, however, simply reflect similar underlying developmental pathways, rather than a co-evolutionary process (10). A recent study using mtDNA sequences (11, 12) challenged some of the earlier conclusions drawn from parsimony analysis of pattern loci. Sequence variation in both species was structured into major geographical regions. Thus, adjacent, often distinct wing pattern races within both species were more closely related than allopatric, but convergent races, indicating that similar patterns within each species had originated independently. Furthermore, the expected phylogenetic signature of co-evolution– that of matching phylogenies between the two species– was not seen. *H. erato* showed a single divide across the Andes, while *H. melpomene* was subdivided into four major biogeographic regions: west of the Andes, the Amazon basin, south-east Brazil, and the Guianan Shield. Given these phylogenetic patterns, Brower (12) concluded that the contemporary wing pattern mosaic arose from several independent mimetic origins. Additionally, based on similar and low levels of mtDNA divergence within the co-mimics, Brower argued that the timeframe of the phenotypic diversification in both species was consistent with of the Pleistocene refuge theory.

Recently there has been renewed interest in the dynamics of Müllerian mimicry and, in particular, the conditions under which co-evolution is expected. Müller's (13) original mathematical formulation clearly demonstrated that, given unequal abundances of two similarly distasteful co-mimics, the rarer species gains a much larger benefit from mimicry than the more abundant species. Thus, in contrast to the mutual convergence implicit in strict co-evolution, the rarer species may evolve, or 'adverge' [sensu (14)], towards the more common species. In order to truly understand the relative roles of each species in the evolution of this parallel diversification we first need to have a clear picture of the historical demographies of the co-mimics. Here we present a comparative historical demographic analysis of *H. erato* and *H. melpomene* using sequence data from two highly variable, unlinked nuclear loci, the autosomal *Mannose phosphate isomerase (Mpi)* and the sex-linked *Triose phosphate isomerase (Tpi)* loci. These data complement the previous mtDNA study of the two species (11, 12), and permit more detailed

insights into the population history of this mimetic association. Genealogical examination across multiple loci is essential in order to distinguish population processes, such as growth or subdivision, from the evolutionary and stochastic forces specific to a single locus.

Methods

We sampled the intron regions of *Mpi* and *Tpi* from ten wing pattern races of *H. erato* and nine of *H. melpomene,* encompassing three major biogeographical regions: W. Andes; E. Andes; and the Guianan Shield (see Supporting Table 1). To place the history of racial diversification within a broader evolutionary context we also sampled the sister species of both radiations. *Heliconius himera* is a geographic replacement of *H. erato* in the dry, elevated forest regions of Southern Ecuador and Northern Peru. *Heliconius cydno* occurs sympatrically with its sister species, *H. melpomene* to the west of the Andes. Although these sister species pairs are known to hybridize in the wild at low (*H. cydno*/*H. melpomene*) to moderate (*H. himera*/*H. erato*) levels, significant behavioral and ecological differentiation warrant species level designations (15, 16). Nonetheless, the exact phylogenetic relationships remain problematic (1). We also sampled outgroup species, *H. clysonimus* and *H. telesiphe* and *H. hecale* (see Supp. Table 1).

DNA sequence data were obtained from *Mpi* and *Tpi* using the methods detailed by Beltrán *et al.* (1). For each individual between three to ten different clones were sequenced in order to identify distinct alleles. Sequences chosen for inclusion were generally represented by at least two identical clones. High substitution rates restricted sequence comparison to closely related species [see (1)], so data were compiled into four distinct alignment files, one for each locus within each radiation (see Supp. Figure 1). Length variation within the numerous small microsatellite repeats were excluded from analyses. Indices of genetic diversity, θ, and recombination, r, were co-estimated using the genealogical, maximum-likelihood approach in the program RECOMBINE v0.4 (17). We used a UPGMA tree generated with PAUP* version 4.0b8 (18) for the initial tree. RECOMBINE was then implemented using 10 short chain runs with a sampling every 40 steps for 2000 steps, followed by a single long chain run, with sampling every 20 steps over a total of 40,000 steps.

Phylogenetic relationships were estimated using Maximum Likelihood (ML) under the heuristic search process in PAUP* version 4.0b8 (18). The best models of DNA substitution were identified using ModelTest 3.06 (19). To identify optimal topologies, an initial ML tree was estimated using tree-bisection-reconnection (TBR) branch swapping routine on the neighbor-joining tree. This tree seeded a second search using nearest-neighbor-interchange (NNI) branch swapping, while re-estimating the most likely substitution parameters. ML topologies were compared to maximum parsimony (MP). The MP was generated using the heuristic search option and TBR reconstruction. The tree used to seed this run was chosen from the the shortest length trees generated during 100 replicates (each running for 2 minutes) of a TBR branch swapping routine run on a tree obtained by random step-wise sequence addition. Confidence within each node was assessed by 500 bootstrap replicates using the heuristic search setting with TBR branch swapping. In an attempt to include the information encoded in insertions and deletions events, each length polymorphism was coded as a single binary character added to the end of the sequence. To test specific phylogenetic relationships between the sister species, the shortest trees representing alternative *a priori* scenarios were generated using MacClade v3.07 (20), starting with the ML trees presented in Figure 1. These topologies were then compared with the ML tree using the method of Shimodaira and Hasegawa (21), implemented in PAUP*.

We explored the partitioning of genetic variation across major geographic boundaries (East Andes, West Andes, Guiana) using two approaches. Firstly, the hierarchical components of sequence variation were estimated at the racial, regional and species level using an analysis of molecular variance (AMOVA), implemented in Arlequin, ver. 2001 (22). Distance matrices were calculated using the best model of DNA substitution. Probabilities were calculated using 20,000 permutations of the data matrix. Secondly, we compared the most parsimonious number of changes needed to explain the geographic location of each allele to the number expected under the null hypothesis of panmixis using the program MacClade v3.07 (20). The expected distribution for the null model was calculated by randomizing geographic location 1000 times.

Finally, we investigated the historical demography of each species using a graphical non-parametric estimate of effective population size, called the generalized skyline plot (23) and evaluated alternative parametric demographic models using GENIE v3.0 (24). Input consisted of ML genealogies first subjected to a non-parametric rate smoothing method (25), with rate differences weighted by the mean at all nodes, as implemented in the program TreeEdit v1.0α10 (http://evolve.zoo.ox.ac.uk).

Results

We sampled 58 and 64 alleles from *Tpi* and *Mpi* respectively in *H. erato*, and 42 and 51 in *H. melpomene*. The two loci showed high intraspecific sequence variation and patterns of variation were consistent with a previous inter-specific study (1). Although recombination may be expected at nuclear loci, levels of *r*, the ratio between per-site recombination rate and per-site mutation rate (17), at *Mpi* and *Tpi* were low in both species, and comparable to those in mtDNA datasets (Table 1). This suggests that the effect of recombination is unlikely to strongly affect phylogenetic or demographic analysis. Consistent with this conclusion was the observation that levels of homoplasy were similar within *Mpi*, *Tpi*, and mtDNA genealogies when the number of taxa were kept constant [data not shown, see also (1)].

At both nuclear loci, *H. erato* possessed much higher levels of variation than *H. melpomene* (Table 1). This difference was unexpected as levels of mtDNA variation in the two species had previously been reported to be roughly equivalent (11, 12). Although our estimate of nucleotide diversity, θ, at mtDNA showed that *H. erato* had higher (but not significantly) levels of diversity than *H. melpomene*, there was some evidence for a reduction in mtDNA diversity within *H. erato*. Assuming that *Mpi* and *Tpi* evolve at roughly the same rate as mtDNA (1) and loci are not under selection, then differences in levels of variation should reflect differences in allelic copy number. Thus, the haploid mtDNA should harbor roughly a third of the variation of the sex-linked *Tpi* locus and a fourth of the variation of the autosomal *Mpi* locus. In *H. melpomene*, this expectation was upheld. However, in *H. erato*, levels of mtDNA variation were 70-80% lower than expected given the observed variation at both nuclear loci.

The differing levels of genetic variation were also partitioned in fundamentally different ways. Within *H. erato*, the vast majority of genetic diversity at both loci was found within the races sampled, and only a very small amount due to regional differences (respectively: 92.85 % versus 2.35% for *Tpi*; 94.56% versus 3.18% for *Mpi*). In contrast within *H. melpomene*, among regional differences explained approximately half of the total variance (51.34% for *Tpi*; 44.18% for *Mpi*). The remaining variance within *H. melpomene* was found within racial populations.

The differences in the levels and distribution of *Tpi* and *Mpi* diversity were clearly evident in the allelic genealogies of the two species. Within *H. erato*, at both loci very similar alleles were distributed broadly across major phenotypic and biogeographic boundaries (Figure 1). At the sex-linked *Tpi* locus, alleles sampled from the sister species, *H. himera*, and those from the geographic race, *H. e. chestertonii*, found in the isolated Cauca Valley of Colombia formed two separate, nested monophyletic lineages. Paraphyly of *H. erato* with respect to *H. himera* was a significantly more likely than reciprocal monophyly of each sister species ($-2\Delta\ln L = 28.1$; df= 14; p= 0.033). At *Mpi*, *H. erato* and *H. himera* were clearly polyphyletic, with *H. himera* falling into two distinctive lineages within the larger *H. erato* genealogy. Despite the lack of a clear phylogeographic signal within *H. erato*, genetic variation at both loci was not distributed randomly and there were differences in the distribution of alleles across the Andes (*Mpi*: p=0.003; *Tpi*: p=0.007, based on randomisation tests): this population structure remains significant with *H. e. chestertonii* alleles excluded.

In contrast, in *H. melpomene* variation in both nuclear loci coalesced broadly into the three major biogeographical regions previously delimited by the mtDNA data (12): West of the Andes;

Amazonia; and the Guianan Shield (Figure 1). At the*Tpi* locus, *H. melpomene* was monophyletic, with *H. cydno* alleles basal and paraphyletic. Although paraphyly of *H. cydno* relative to *H. melpomene* was the most likely model, neither reciprocal monophyly or polyphyly could be rejected [data not presented; see (1)]. At *Mpi*, the genealogical pattern was more complex, with *H. melpomene* and *H. cydno* sharing very similar alleles. Nonetheless, three major regional clades in *H. melpomene* were clearly identifiable (Figure 1B). Within both nuclear genealogies there were several exceptions to this geographic structure. For example, at the *Mpi* locus, alleles sampled from the Guianan shield fell into two clades. One consisted of only alleles found on the Guiana Shield, and the other formed a single derived lineage within a clade of alleles sampled from the Amazonian region. These inconsistencies, however, may be explained by a small number of migration events.

The pattern of coalescent events in the *Tpi* and *Mpi* genealogies further highlighted differences in the evolutionary history of the two co-mimics. In both species, genealogies were most consistent with a history of population growth rather than constant effective population size (Table 2; Figure 2). However, the processes shaping the demographic histories operated over very different time scales. In *H. erato*, assuming approximately clock-like evolution and a evolutionary rate comparable to the mitochondrial COI/COII region [1% sequence divergence per lineage per Myrs (11)] (1), the time to most recent common ancestor (TMRCA) at both loci occurred within the Pliocene (Figure 2). Since that time, the genealogies of both nuclear loci was most consistent with population growth, both across the species and within major biogeographic regions (Table 2). In contrast, for *H. melpomene*, assuming the same substitution rate the TMRCA was much more recent at both *Tpi* and *Mpi*., occurring near the Pliocene/Pleistocene boundary. Nonetheless, there was similar evidence for population growth (Table 2). In this case, regional population growth was likely to have occurred within the latter half of the Pleistocene: average pairwise differences within regional clades ranged from 0.52-0.55% (uncorrected) at *Mpi* and 0.53-1.1% (uncorrected) at *Tpi*, suggesting these independent population expansions began roughly 250,000-500,000 years ago.

Discussion

Our understanding of the evolutionary history of the parallel mimetic radiations within *H. erato* and *H. melpomene* is significantly enhanced by the addition of high-resolution genealogical information for two unlinked nuclear loci. Consistent with the previous mtDNA study (11, 12), the phylogeographic patterns at the nuclear loci were not concordant between the co-mimics. However, in marked contrast to the mtDNA data, genealogical and coalescent-based analyses of nuclear loci clearly showed that the two co-mimics have had very different demographic histories over the period in which racial diversification is speculated to have evolved. In *H. erato,* considerable variation at *Tpi* and *Mpi* revealed high levels of historical gene flow across the species' range and suggests that population expansion occurred throughout the Pleistocene. Levels of variation at both nuclear loci were much lower in *H. melpomene* and were partitioned into three major geographical regions. Distribution of coalescent events indicated population expansion occurred independently within each region and over a much more recent time period than that of *H. erato*. These contrasting evolutionary and demographic patterns suggest that racial diversification did not occur simultaneously, and challenge the Pleistocene refuge theory for the origins of this extraordinary mimetic radiation (8, 12).

Evolutionary and demographic history of **H. erato**.

The nuclear data argue for a significantly different population history in *H. erato* relative to that previously envisioned from mtDNA, highlighting the importance of using multi-locus comparisons to infer the population and demographic history of a species (26). Mitochondrial DNA variation in *H. erato* was partitioned into two regional clades separated by the Andes (11). Very low levels of intra-clade mtDNA variation suggested that racial diversification had evolved recently (within the last 200,000 years), broadly consistent with the Pleistocene refuge theory for wing pattern radiation (11, 12).

The nuclear sequence data, in contrast, did not show a marked genetic discontinuity across the Andes, nor any evidence for historic population constrictions, as predicted by the refuge hypothesis. Both nuclear genealogies indicated historically high levels of gene flow across the entire range of *H. erato* and population expansion throughout the Pleistocene. There was evidence for genetic differentiation between *H. erato* populations separated by the Andes, which today pose a formidable barrier to dispersal for these low-mid elevation tropical butterflies. However, these patterns are more consistent with the gradual accumulation of genetic differences between recently isolated populations, than with the population constrictions predicted by the refuge hypothesis. The close association of nuclear alleles sampled from either side of the Andes likely reflects the shared history prior to the establishment of the Andes as a significant barrier to gene flow.

The phylogenetic discrepancies between the nuclear and mtDNA data may reflect differences in expected coalescence times for the different loci. However, levels of mtDNA diversity within *H. erato* were much lower than expected based on extant levels of variation at both *Tpi* and *Mpi* (Table 1). It is unclear whether low mtDNA diversity is a sampling artifact, reflects stochastic lineage extinction, or is the result of purifying selection on mtDNA. Nonetheless, the agreement between the two unlinked nuclear loci suggests that genealogical patterns at these loci better reflect historical demographics within *H. erato*. Furthermore, lack of evidence for Pleistocene population constrictions in *H. erato* is concordant with accumulating palynological data. Contrary

to the hypothesis of allopatric forest refugia, recent paleoecological studies indicate that continuous tropical forest likely persisted in the Amazon region across the Pleistocene climatic fluctuations (27).

This scenario of a broad panmictic population predating the rise of the Andes also conflicts with previous ideas regarding the origin of *H. erato*. Brower (11, 12) hypothesized that *H. himera*, with its trans-Andean distribution, had provided the source for separate *H. erato* wing pattern radiations East and West of the Andes. Given average pairwise mtDNA divergences between *H. erato* and *H. himera* of around 3% (1, 11), this would place the origin of *H. erato* in the early Pleistocene. However, paraphyly of *H. erato* relative to *H. himera* now indicates that the divergence between these supposed sister species is not an appropriate node on which to date the origin of *H. erato*. In contrast, average uncorrected pairwise divergences between *H. erato* and the two most closely related species sampled, *H. clysonimus* and *H. telesiphe*, are approximately 5% at the mtDNA and *Tpi* loci respectively (1, 11), taking the origin of *H. erato* back into the Pliocene. Coalescent-based analyses support this earlier origin, placing the TMRCA for the high levels of extant variation at both nuclear loci in the mid-late Pliocene (Figure 2). Additionally, Brower's hypothesis predicts a phylogenetic split between the eastern and western ranges of *H. himera* in S. Ecuador and N. Peru respectively, which we did not observe at either *Mpi* or *Tpi*. A more likely evolutionary scenario is that *H. himera*, with a restricted, elevated distribution, evolved from a peripherally isolated wing pattern variant within a widely-distributed *H. erato* lineage. Our nuclear alleles from *H. himera* show surprisingly low levels of divergence, falling within a single, well differentiated lineage at the *Tpi* loci, and two lineages (but not East and West) at the *Mpi* locus, as predicted by a peripheral isolate or 'peripatric' speciation model (Figure 1). The race, *H. e. chesteronii* displays a similar phylogenetic pattern. Like *H. himera*, this race occurs in an ecologically differentiated, elevated region, lacks a *H. melpomene* co-mimetic race, and may also represent a peripatric divergence event.

***Evolutionary and demographic history of* H. melpomene.**

In *H. melpomene*, the mtDNA (12), *Tpi*, and *Mpi* gene genealogies were largely concordant and supported a very different population history for this species relative to its co-mimic. Variation at all three loci was low (Table 1) and placed the TMRCA within the first half of the Pleistocene (Figure 2). This approximate date was consistent with estimates of divergence time between *H. melpomen*e and *H. cydno* (1). Thus, unlike in *H. erato*, both extant levels of intraspecific diversity and estimates of divergence time place the origin of the *H. melpomene* lineage within the Pleistocene.

Furthermore, all three loci demonstrate clear population fragmentation over the Pleistocene. Genetic variation was divided into major biogeographical regions, but the phylogenetic relationships among regional clades varied depending on which locus was used. For example, the Guiana Shield lineage was an outgroup to the rest of the *H. melpomene* radiation for mtDNA (12) but was the most derived lineage at *Tpi* (Figure 1A). At *Mpi*, all three lineages were equally divergent (Figure 1B). These inconsistencies likely reflect the stochastic fixation of ancestral variation within emerging regional clades, and suggest that the clades were formed roughly simultaneously, early in the evolution of *H. melpomene* lineage. Both of the two main color pattern types, 'rayed' and 'banded', occur in more than one of the geographical lineages identified

in *H. melpomene,* supporting Brower's contention that similar color patterns have evolved independently within each biogeographic region (12).

This Pleistocene subdivision was associated with changes in the population dynamics of the emerging geographic lineages. The individual clades at both nuclear loci for *H. melpomene* were characterized by low levels of variation relative to that of the entire species sample (Figure 1), suggesting a loss of variation, possibly as a consequence of population constrictions in each region. Additionally, the star-like nature of the genealogies of the *H. melpomene* clades, resulting from a high frequency of singleton mutations between these alleles, is highly characteristic of recent population expansion. Furthermore, despite small sample sizes and low levels of sequence variation, models of historical population growth were supported over constant population size in all geographical regions, at both nuclear loci (Table 2). At *Mpi,* demographic analysis was complicated by polyphyly of *H. melpomene* and *H. cydno* (Figure 1B). A more extensive sampling of both species in areas of sympatry suggests that introgressive hybridisation most likely generated this phylogenetic pattern (Bull *et al.*, submitted). Removing alleles of probable hybrid origin (* in Figure 1B) greatly strengthens support for a recent history characterized by rapid population growth ($2\Delta\ln$ for constant versus logistic = 49.8, p= 0.0000, df= 1). Interestingly, these strong genealogical and demographic trends are coupled with the evolution of significant postzygotic hybrid sterility between geographical regions of *H. melpomene* (15), in contrast to the lack of postzygotic reproductive isolation among races of *H. erato* (8).

***Advergence and the evolution of mimicry between* H. erato *and* H. melpomene.**

We found no evidence that the two co-mimics shared similar demographic histories, as predicted by the Brown-Sheppard-Turner co-evolution model. Instead, our data strongly suggest that the phenotypic diversity in *H. erato* arose first and *H. melpomene* radiated subsequently to mimic *H. erato*, a scenario first proposed by Elthringham early in the 20th Century. Eltringham (6, 28) noted that *H. erato* was almost always much more common that *H. melpomene*, an observation borne out by 90 years of subsequent field research (6). Based on differences in relative abundances, he argued that *H. erato* was the model for the mimetic association, and that *H. melpomene* had evolved unilaterally to mimic *H. erato*. As Eltringham recognized, the number-dependent selection proposed by Müller (13) provides a potent driving force for this mimetic advergence. The relative gain due to Müllerian mimicry between similarly unpalatable species is proportional to the square of the ratio of their relative abundances. Thus, the rarer species gains considerably more from mimicry than the common species. Our data support Eltringham's mimetic advergence hypothesis in several ways. The much higher levels of variation in *H. erato* relative to *H. melpomene* at both *Mpi* and *Tpi* are consistent with a larger historical effective population size in *H. erato*. Moreover, plots of the effective population size through time indicate that this demographic difference has persisted over both species' histories (Figure 2). Additionally, our analyses indicate that *H. erato* is the older lineage, predating the origins of the *H. melpomene* lineage by some 1-2 million years. Finally, the likely peripatric differentiation of both *H. himera* and *H. e. chestertoni* suggest that the phenotypic radiation in *H erato* may have evolved quite early in the history of the species.

Although Eltringham (28) did not articulate how he envisioned the initial wing pattern radiation in *H. erato* to have occurred, wing pattern radiation would not necessarily require allopatry (5). Recent empirical research has shown that the selection against novel wing patterns is extremely

sensitive to changes in density (29). Thus, even a relatively small number of novel-patterned, distasteful butterflies can educate potential predators. If the novel phenotype reaches a critical density or occupies a critical radius, selection will cause the two warning patterns to be separated by a steep cline (5). These clines are unstable and will spread (30), but can become trapped in regions of low density, at boundaries between ecotones, or other physical barriers to gene flow (5, 30). Hybrid zones between races will permit introgression at most loci not closely linked to those determining wing pattern differences; the high levels of gene flow detected across contemporary hybrid zones between parapatric races (J. Mallet; N.S. Flanagan, unpublished data) is consistent with this prediction. The establishment of novel pattern variation in *H. erato* in this manner could then easily drive mimetic advergence in *H. melpomene*. Indeed, with the five-fold difference in abundances suggested by the nuclear data, and often observed in real populations (6, 29), *H. melpomene* would receive 25-times more benefit from mimicry than *H. erato*. A newly formed *H. melpomene* pattern would quickly spread to occupy the range of its model, generating the parallel color-pattern mosaic that we observe today (30).

The differing evolutionary and demographic histories revealed from analysis of nuclear data now indicate that a simultaneous diversification of *H. erato* and *H. melpomene* wing patterns is unlikely. Instead, the older origin, greater abundances, and earlier population expansion in *H. erato* suggest that the wing pattern radiation occurred first in this species and that diversification in *H. melpomene* evolved through advergence. Nonetheless, the suggestion that the wing pattern radiation in these butterflies evolved in concert cannot be unequivocally rejected. The wing patterns of *Heliconius* butterflies are remarkably labile, as evidenced by the rapid, independent diversification of wing pattern variation within regional clades of *H. melpomene*. Extremely strong selection acts on the relatively small number of loci that control wing pattern variation (10), providing the opportunity for continual mimetic evolution under some conditions. It is therefore possible that our estimation of the ‘average’ historical demography of these species does not directly reflect the specific demographic conditions under which wing patterns evolved. A definitive answer awaits comparative phylogenetic analysis of the color pattern loci themselves, a very real future possibility as genetic mapping work progresses (Tobler et al., pers. comm.) and genomic resources for *Heliconius* butterflies expand (31).

Acknowledgements.
We are indebted to Margarita Beltran, Chris Jiggins and Jim Mallet for sharing samples, and to Chris Jiggins, Tupac Otero and Shannon Bennett for valuable discussions. We thank Germania Estévez in Ecuador, and Courtney Rooks and The Paria Springs Eco-Community in Trinidad for help with collections. We are also grateful to the Autoridad Nacional del Ambiente in Panama and the Ministerio del Ambiente in Ecuador for permission to collect butterflies. Funding was provided by NSF (WOM and DH), the PR-EPSCoR program (NSF and WOM), and the Wellcome Trust (OGP).

Figure 1. Maximum-likelihood genealogies for *H. erato* and *H. melpomene* of *Tpi* alleles (A), and *Mpi* alleles (B). Best models of evolution were: TrN+I+G, *P*(I) =0.3402, a =0.8850 for *Tpi H. erato*; TrN+I, *P*(I) = 0.6301 for *Tpi H. melpomene*; GTR+G, a = 0.6013 for *Mpi H. erato;* and TrN+I, *P*(I) = 0.4376 for *Mpi H. melpomene*. MP genealogies were qualitatively and quantitatively similar. Numbers on the branches are parsimony bootstrap values for the equivalent nodes on the ML tree. Sequences are labeled with a racial code, individual number, allele identity (A or B), and country code (see Supp. Table 1).
Racial identity codes for *H. erato* were: CHE– *H. e. chesteronii*; CYR– *H. e. cyrbia*; EMM– *H. e. emma*; ERA– *H. e. erato*; ETY– *H. e. etylus*; FAV – *H. e. favorinus*; HYD – *H. e. hydara*; LAT– *H. e. latavitta*; NOT– *H. e. notabilis*; PET– *H. e. petiverana*; HIM – *H. himera*. Racial identity codes for *H. melpomene* were: AGLA– *H. m. aglaope*; MALL- *H. m. malleti;* AMAR– *H. m. amaryllis*; CYTH – *H. m. cythera*; ECUA– *H. m. ecuadoriensis*; MELP *H. m. melpomene*; PLES–*H. m. plessini*; ROSI– *H. m. rosina*; THEL– *H. m. thelxiopeia*. Country codes are as follows: Pe– Peru; EcW– Ecuador, western slope of Andes; EcE– Ecuador, eastern slope of Andes; Pa– Panama; Co– Colombia; TT– Trinidad and Tobago; FG– French Guiana. In B, *H. melpomene* alleles marked with an asterisk are hypothesized to be of hybrid origin based a larger sampling of alleles (Bull *et al*, submitted).

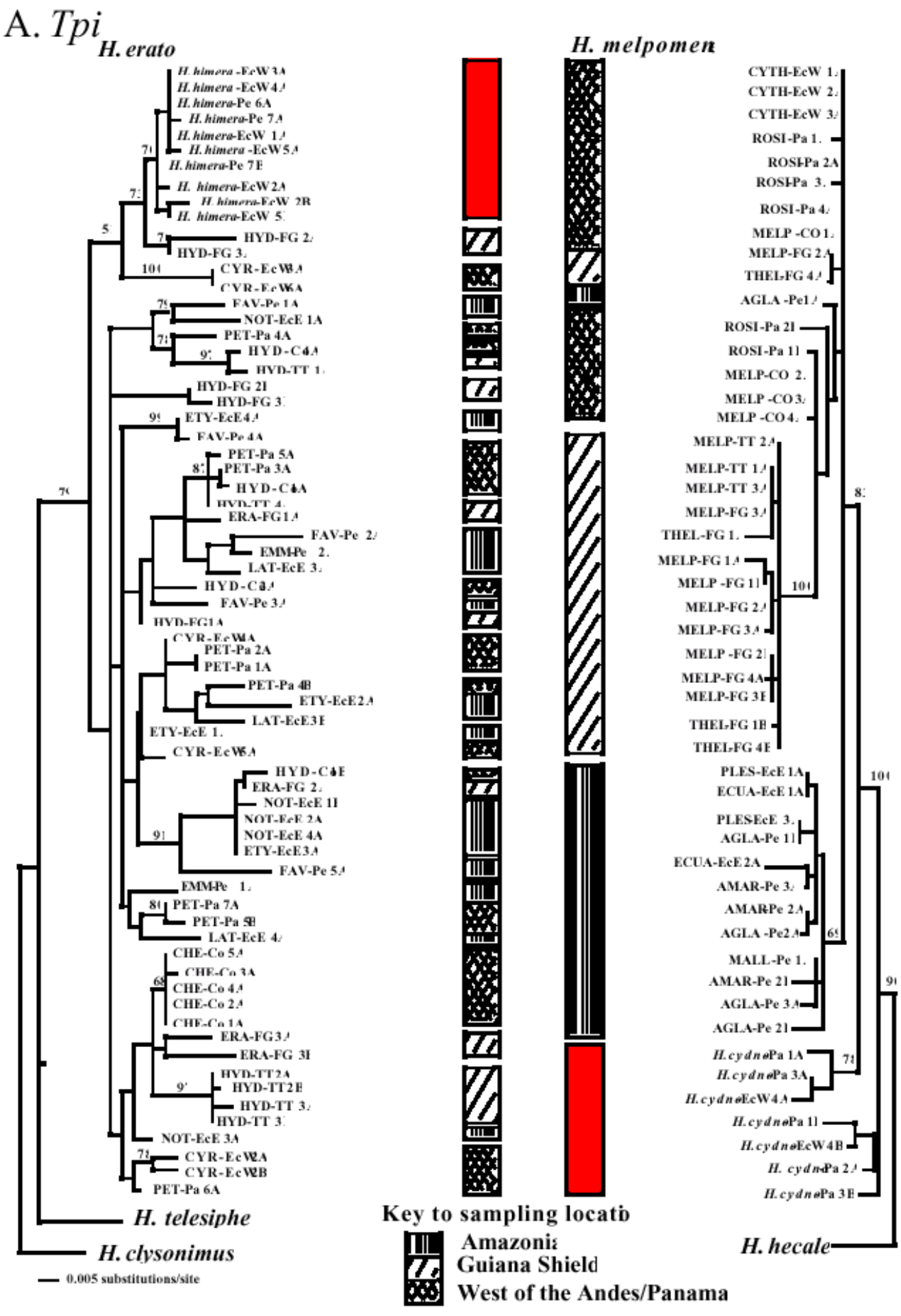
A. Tpi
H. erato
H. melpomene
H. telesiphe
H. clysonimus
H. hecale
0.005 substitutions/site
Key to sampling locati
Amazonia
Guiana Shield
West of the Andes/Panama

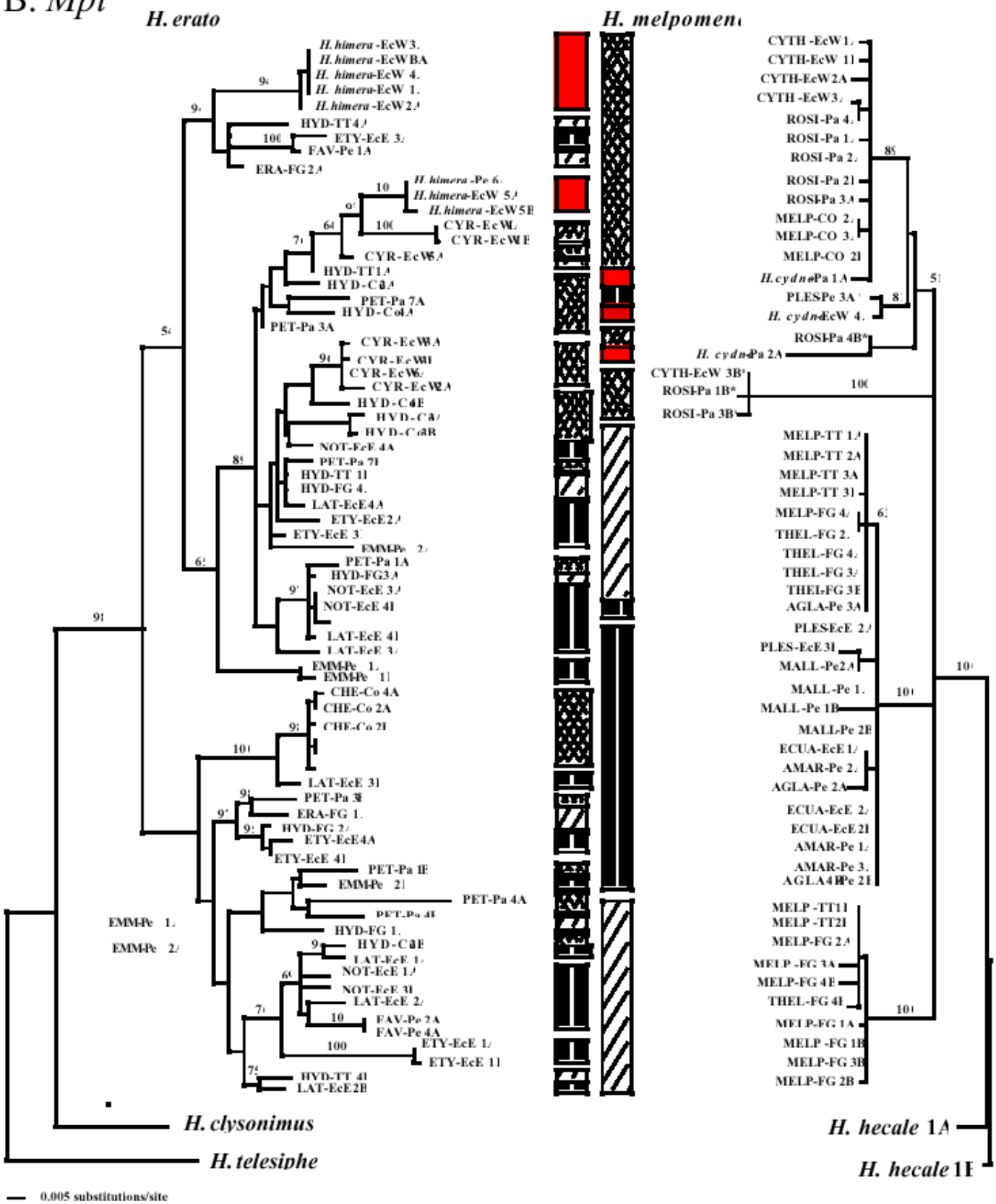
B. Mpi
H. erato
H. melpomen
H. himera -EcW3.
H. himera -EcWBA
H. himera-EcW 4.
H. himera-EcW 1.
H. himera -EcW2A
HYD-TT4A
ETY-EcE 3.
FAV-Pe 1A
ERA-FG 2A
H. himera -Pe 6.
H. himera-EcW 5A
H. himera -EcW5E
CYR-EcW.
CYR-EcW.E
CYR-EcW5A
HYD-TT1A
HYD-CoA
PET-Pa 7A
HYD-CoA
PET-Pa 3A
CYR-EcW8A
CYR-EcW8
CYR-EcW6.
CYR-EcW2A
HYD-C4E
HYD-CoA
HYD-CoB
NOT-EcE 4A
PET-Pa 7E
HYD-TT 1E
HYD-FG 4.
LAT-EcE4A
ETY-EcE2A
ETY-EcE 3.
EMM-Pe 2.
PET-Pa 1A
HYD-FG3A
NOT-EcE 3A
NOT-EcE 4E
LAT-EcE 4E
LAT-EcE 3.
EMM-Pe 1.
EMM-Pe 1E
CHE-Co 4A
CHE-Co 2A
CHE-Co 2E
LAT-EcE 3E
PET-Pa 3E
ERA-FG 1.
HYD-FG 2.
ETY-EcE4A
ETY-EcE 4E
PET-Pa 1E
EMM-Pe 2E
PET-Pa 4A
PET-Pa 4E
EMM-Pe 1.
EMM-Pe 2.
HYD-FG 1.
HYD-CoE
LAT-EcE 1.
NOT-EcE 1A
NOT-EcE 3E
LAT-EcE 2.
FAV-Pe 2A
FAV-Pe 4A
ETY-EcE 1.
ETY-EcE 1E
HYD-TT 4E
LAT-EcE2E
CYTH -EcW1.
CYTH-EcW 1E
CYTH-EcW2A
CYTH -EcW3.
ROSI-Pa 4.
ROSI-Pa 1.
ROSI-Pa 2.
ROSI-Pa 2E
ROSI-Pa 3A
MELP-CO 2.
MELP-CO 3.
MELP-CO 2E
H.cydnoPa 1A
PLESPe 3A
H. cydnoEcW 4.
ROSI-Pa 4B*
H. cydnoPa 2A
CYTH-EcW 3B*
ROSI-Pa 1B*
ROSI-Pa 3B*
MELP-TT 1A
MELP-TT 2A
MELP-TT 3A
MELP-TT 3E
MELP-FG 4.
THEL-FG 2.
THEL-FG 4.
THEL-FG 3.
THEL-FG 3E
AGLA-Pe 3A
PLES-EcE 2.
PLES-EcE3E
MALL-Pe2A
MALL-Pe 1.
MALL-Pe 1B
MALL-Pe 2E
ECUA-EcE 1.
AMAR-Pe 2.
AGLA-Pe 2A
ECUA-EcE 2.
ECUA-EcE 2E
AMAR-Pe 1.
AMAR-Pe 3.
AGLA4BPe 2E
MELP -TT1E
MELP -TT2E
MELP-FG 2A
MELP -FG 3A
MELP-FG 4E
THEL-FG 4E
MELP-FG 1A
MELP -FG 1E
MELP-FG 3E
MELP-FG 2B
H. clysonimus
H. telesiphe
H. hecale 1A
H. hecale 1E
0.005 substitutions/site

Figure 2. Estimated demographic histories of the *H. erato* and *H. melpomene* radiations, for (A) *Tpi* and (B) *Mpi*. The thicker, piecewise plots are the generalized skyline plots, a non-parametric estimate of effective population size through time. The thinner, smooth curves represent the parametric ML demographic history (see Table 2). Plots for *H. erato* (green) and *H. melpomene* (blue) are shown on the same graph.

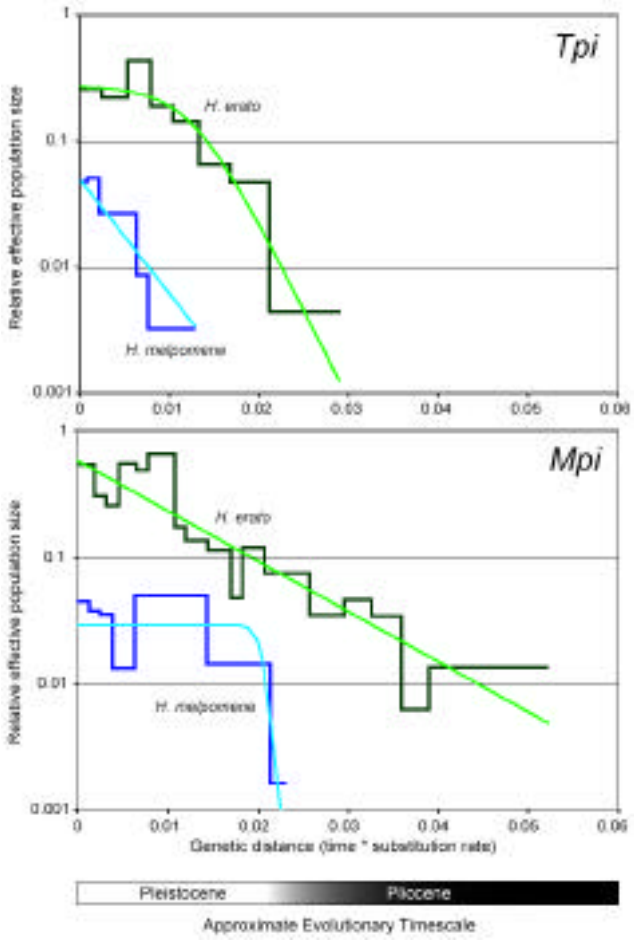
Tpi
H. erato
H. melpomene
Relative effective population size
1
0.1
0.01
0.001
0
0.01
0.02
0.03
0.04
0.05
0.06
Mpi
H. erato
H. melpomene
Relative effective population size
Genetic distance (time * substitution rate)
Pleistocene
Pliocene
Approximate Evolutionary Timescale

1

Table 1. Estimates of genetic diversity (θ) and recombination (r) (15) for mtDNA, *Tpi*, and *Mpi* in *H. erato* and *H. melpomene* with approximate 95% confidence intervals (CIs). Estimates for the mtDNA were derived using previously published sequence data (8, 9), pruned to include only the geographic samples corresponding to those available for *Mpi* and *Tpi*.

Species	Locus	n	θ (95% CI)	*r* (95% CI)
H. erato	*mtDNA*	31	0.05 (0.03 - 0.08)	0.00 (0.00 - 0.14)
	Tpi	58	0.27 (0.19 - 0.38)	0.01 (0.00 - 0.04)
	Mpi	64	0.38 (0.28 - 0.53)	0.00 (0.00 - 0.01)
H. melpomene	*mtDNA*	22	0.02 (0.01 - 0.04)	0.00 (0.00 - 0.00)
	Tpi	42	0.06 (0.03 - 0.09)	0.00 (0.00 - 0.04)
	Mpi	51	0.08 (0.05 - 0.11)	0.00 (0.00 - 0.04)

Table 2. Evaluation of alternative parametric demographic models for the genealogies of *H. erato (*excluding *H. e. chestertonii)* and *H. melpomene,* and their sub-populations, at *Mpi* and *Tpi*. The most likely model was compared to constant and exponential models (* = $p<0.05$; ** = $p<0.01$). For *H. melpomene* results are presented with alleles of likely hybrid origin with *H. cydno* (see figure 1) excluded from the analysis. An expansion growth model never gave a better fit, and results are not presented.

Species	Locus	Sample	n	Highest Likelihood Model	Reject Constant Model?	Reject Exponential Model?
H. erato	*Tpi*	All	53	logistic	Yes**	Yes**
		West	19	logistic	Yes**	Yes**
		East	34	logistic	Yes**	Yes**
	Mpi	All	61	logistic	Yes**	No
		West	24	logistic	Yes**	Yes**
		East	37	logistic	Yes**	No
H. melpomene	*Tpi*	All	42	logistic	Yes**	No
		West	13	logistic	Yes**	Yes**
		East	13	logistic	Yes**	No
		Guiana	16	logistic	Yes*	Yes*
	Mpi	All	48	logistic	Yes*	Yes**
		West	13	logistic	Yes*	No
		East	16	log/expo	Yes**	No
		Guiana	19	logistic	Yes**	Yes**

Bibliography.

1. Beltrán, M., Jiggins, C. D., Bull, V., Linares, M., Mallet, J., McMillan, W. O. & Bermingham, E. (2002) *Molecular Biology and Evolution* **19,** 2176-2190.
2. Brower, A. V. Z. (1994) *Molecular Phylogenetics and Evolution* **3,** 159-174.
3. Benson, W. W. (1972) *Science* **176,** 936-939.
4. Mallet, J. & Barton, N. H. (1989) *Evolution* **43,** 421-431.
5. Turner, J. R. G. & Mallet, J. L. B. (1996) *Philosophical Transactions of the Royal Society of London B Biological Sciences* **351,** 835-845.
6. Mallet, J. (2001) *Evolutionary Ecology* **13,** 777-806.
7. Haffer, J. (1969) *Science* **165,** 131-137.
8. Sheppard, P. M., Turner, J. R. G., Brown, K. S., Benson, W. W. & Singer, M. C. (1985) *Philosophical Transactions of the Royal Society of London B Biological Sciences* **308,** 433-613.
9. Brown, K. S., Sheppard, P. M. & Turner, J. R. G. (1974) *Proceedings of the Royal Society London, B Biological Sciences* **187,** 369-387.
10. Nijhout, H. F. (1991) *The Development and Evolution of Butterfly Wing Patterns* (Smithsonian Institute Press, Washington).
11. Brower, A. V. Z. (1994) *Proceedings of the National Academy of Science U.S.A.* **91,** 6491-6495.
12. Brower, A. V. Z. (1996) *Evolution* **50,** 195-221.
13. Müller, F. (1879) *Transactions of the Entomological Society of London* **1879,** xx-xxix.
14. Brower, L. P., Brower, J. V. Z. & Collins, C. T. (1972) in *Ecological Essays in Honour of G. Evelyn Hutchinson*, ed. Deevey, E. (Connecticut Academy of Arts and Sciences, Connecticut), pp. 57-67.
15. Jiggins, C. D., Naisbit, R. E., Coe, R. L. & Mallet, J. (2001) *Nature* **411,** 302-305.
16. McMillan, W. O., Jiggins, C. D. & Mallet, J. (1997) *Proceedings of the National Academy of Science U.S.A.* **94,** 8628-8633.
17. Kuhner, M. K., Yamato, J. & Felsenstein, J. (2000) *Genetics* **156,** 1393-1401.
18. Swofford, D. L. (2000) (Sinauer Associates, Sunderland, MA).
19. Posada, D. & Crandall, K. A. (1998) *Bioinformatics* **14,** 817-818.
20. Maddison, W. P. & Maddison, D. R. (1997) (Sinauer Associates, Sunderland, MA).
21. Shimodaira, H. & Hasegawa, M. (1999) *Molecular Biology and Evolution* **16,** 1114-1116.
22. Schneider, S., Roessli, D. & Excoffier, L. (2000), Genetics and Biometry Laboratory, University of Geneva, Switzerland).
23. Strimmer, K. & Pybus, O. G. (2001) *Molecular Biology and Evolution* **18,** 2298-2305.
24. Pybus, O. G. & Rambaut, A. (2002) *Bioinformatics* **18,** 1404-1405.
25. Sanderson, M. J. (1997) *Molecular Biology and Evolution* **14,** 1218-1231.
26. Edwards, S. V. & Beerli, P. (2000) *Evolution* **54,** 1839-1854.
27. Colinvaux, P. A. & Oliveira, P. E. D. (2001) *Palaeogeography, Paleoclimatology, Palaeoecology* **166,** 51-63.
28. Eltringham, H. (1916) *Transactions of the Entomological Society of London* **1916,** 101-148.
29. Kapan, D. D. (2001) *Nature* **409,** 338-340.
30. Sasaki, A., Kawaguchi, I. & Yoshimori, A. (2002) *Theoretical Population Biology* **61,** 49-71.

31. Couzin, J. (2003) *Science* **297,** 1638-1639.